COMMUNICATIONS IN SCIENCE AND TECHNOLOGY
Homepage: cst.kipmi.or.id

A review of measurement of electromagnetic emission in electronic product: Techniques and challenges

Tito Yuwono[a,b], Mohd Hafiz Baharuddin[a,*], Norbahiah Misran[a], Mahamod Ismail[a], Mohd Fais Mansor[a]

[a] *Department of Electrical, Electronic, and System Engineering, Universiti Kebangsaan Malaysia, 43600, Bangi, Malaysia*
[b] *Department of Electrical Engineering, Islamic University of Indonesia, 55584, Yogyakarta, Indonesia*

Article history:
Received: 22 February 2022 / Received in revised form: 25 May 2022 / Accepted: 30 May 2022

Abstract

Nowadays, electronic products are being used extensively in many fields and applications. The dense population of electronic devices in human life has become a challenge for microwave engineers to ensure that their products can meet the Electromagnetic Compatibility (EMC) standards. Complex electronic products with smaller sizes and denser components will be a challenge for compliance with EMC standards. In addition, the occurrence of non-stationary emission at certain operating modes becomes a challenge for analysis. Error in analyzing EM emissions will make the products unable to meet the requirements of EMC standards; hence, they will be prohibited to be marketed. Currently, there are two methods of emission analysis, i.e. by measurement and modeling or computation. There are some problems, however, in the analysis of EM emissions regarding the area of test, complexity, DUT positioning error, installation cost, and time consumption. In this paper, the analysis techniques for EM emissions including Open Area Test Site (OATS), Anechoic chamber, Transverse Electromagnetics TEM Cell, Compact Antenna Test Range (CATR) and near field scanning are reviewed comprehensively. This survey covered EMC standards, principles of EM emission measurement techniques, advantages and disadvantages of EM emission measurement techniques, studies and applications of each technique, recommendations for which technique to be used, and challenges for future research in EM emission measurement. The final section of this paper discusses the challenges for near-field measurements related to the non-stationary emissions phenomenon. This papers also presents the challenges of how to detect and characterize them.

Keywords: EM emission; EMC; measurement; electronic product

1. Introduction

Technically, an electronic product must meet functional requirements and Electromagnetic Compatibility (EMC) compliance requirements prior to be commercialized. Functional requirements mean that the electronic product must properly function according to the purpose of the product being made, while EMC requirements means that the EM emissions of the electronic product must meet the requirements of international regulations and standards related to EMC. EM emission fulfillment is one of the EMC provisions to guarantee the ability of an electronic product to work properly without affecting or causing interference to the electronic products nearby. Compliance to these standards is critical to prevent electromagnetic emission pollution [1], which is known as electromagnetic interference (EMI) [2].

An important aspect of modern electronic products is unpredictable emissions that are potential to cause interference to other electronic products [3]. The Electromagnetic Interference (EMI) can reduce the performance of the surrounding electronic products. Hence, it is not allowed the EMI emission of a product to exceed the threshold of the standard. If it exceeds the threshold, the functionality of neighbouring electronic products will most likely be degraded [3].

The advancement in the field of electronic products in recent years has resulted in integration of many components of the communication platform in a PCB. In addition, the IoT era has increased the complexity of electronic systems, including intelligent surveillance system [4]. The extensive development and application of IoT with a support of 5G technology will bring an impact on the increase of the mass of consumer devices, highly congested locations, and flexible and dynamic frequency bands. This development will contribute to the EMC problem. Then, it becomes a challenge to develop EMC measurement and analysis for future technologies [5]. According to the International Electrotechnical Commission (IEC) glossary, EMC is defined as the ability of an electronic product to perform properly in its electromagnetic environment, and not to cause electromagnetic interference to other products [6].

* Corresponding author.
Email: hafizb@ukm.edu.my
https://doi.org/10.21924/cst.7.1.2022.727

Electronic products can meet EMC requirements if they have the following requirements [3,7,8]: (i) not causing interference to other systems; (ii) having resistance to emissions from other systems; and (iii) not causing interference to the product itself technically.

Electromagnetic emission measurement of the electronic product is a critical activity to ensure that the product meets EMC standards. There are several techniques commonly used, including Open Area Test Site (OATS), Anechoic Chamber (AC), Reverberation Chamber (RC), Transverse Electromagnetic (TEM/GTEM) cell, and Near Field Scanning (NFS). This paper presents a comprehensive review of measurement of electromagnetic emissions in electronic products. It consists of five sections in which the first section presents an introduction discussing the importance of EMC and measurement for analyzing emissions in general. The second one presents the established EMC standards and the third one presents the techniques for measuring electromagnetic emissions in detail. The fourth and fifth section respectively present discussion and recommendation, and conclusions and future study related to more effective emission analysis techniques. Table 1 presents a list of acronyms to make it easier to understand the acronyms used in this paper.

Table 1. List of acronyms in this text

Acronym	Stand
AC	Anechoic Chamber
CATR	Compact Antenna Test Range
CISPR	Comité International Spécial des Perturbations Radioélectriques
DUT	Device Under Test
EMC	Electromagnetic Compatibility
EMI	Electromagnetic Interference
FCC	Federal Communication Commission
FPGA	Field Programmable Gate Array
IEC	International Electrotechnical Committee
MIU	Measurement Instrumentation Uncertainty
NFS	Near Field Scanning
OATS	Open Area Test Site
PCB	Printed Circuit Board
RC	Reverberation Chamber
TEM cell	Transverse Electromagnetic cell

2. EMC Standards

The most widely used EM emission standards for electronic products in the world are CISPR and FCC. Generally, the CISPR standard is adopted outside America, while the FCC one is an EM emission regulation in America. In French, the term of CISPR stands for Comité International Spécial des Perturbations Radioélectriques [9]. The CISPR has been established by several international organizations to determine the measurement methods and limits for radio frequency interference. Since 1950, it has become a special committee under International Electrotechnical Committee (IEC). The FCC meanwhile has handled EMC since 1934 [9]. In that year it was authorized by the Communications Act to enforce rules and regulations on industrial, commercial, and consumer devices that can emit electromagnetic energy. The FCC classifies electronic products into two classes: Class A and Class B. Class A are the electronic products for industrial, scientific and medical applications, while Class B is for the electronic product applications in residential environments. Generally, class B standards are stricter than that of class A. Figure 1 shows the emission limits for Class A and Class B according to the FCC [10]. Here, measurements have been made with a distance of 3 meters.

The emission standards based on CISPR (CISPR 22) are also divided into Class A and Class B. Figure 2 shows the emission maximum limits for class A and class B according to CISPR 22 [11]. Measurements here have been made with a distance of 10 meters.

In CISRP 22, the measurement distance between the DUT and the antenna receiver is always 10 meters. In FCC, the distance between the DUT and the receiving antenna is 10 meters for class A and 3 meters for class B. Thus, to get the value of the electric field within 10 meters from the value of the electric field within 3 meters for class A, it is reduced by a factor of 3/10.

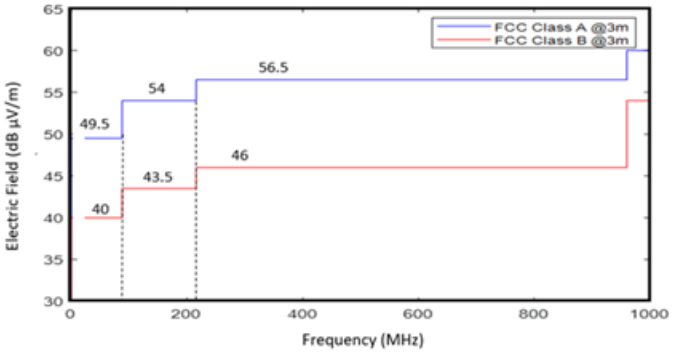

Fig. 1. EMC based FCC Standard

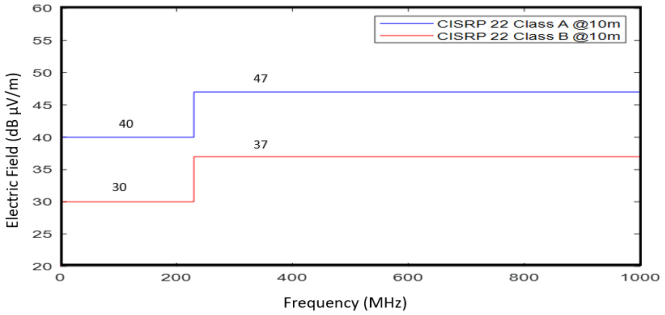

Fig. 2. EMC based CISRP 22 Standard

3. EM Emission Measurement Techniques

Currently, there are several techniques for measuring the EM emission of electronic products. Some of these techniques include Open Area Test Site (OATS), Anechoic Chamber (AC), Compact Antenna Test Range (CATR), Transverse Electromagnetic (TEM) cells, Reverberation Chamber (RC), and Near Field Scanning (NFS). The selection of this measurement technique depends on the signal strength, device dimensions, working frequency and resource availability.

3.1. OATS

OATS is a measurement technique of EM emissions in an open space. It is commonly used to measure the far field of antennas and for antennas calibration. In addition, OATS is an EM emission testing technique defined by EN 55032 [12], as shown in Figure 3. The Device Under Test (DUT) is placed with distance r from the receiver antenna. The requirement of the far-field measurement is that r is greater than $2D^2/\lambda$ [13]. This receiver antenna has several radiation characteristics such as gain and radiation pattern. For the emission test using OATS,

DUT functions as a transmitter and antenna as a receiver. While for the immunity test, the DUT is functioned as a receiver and the antenna as a transmitter.

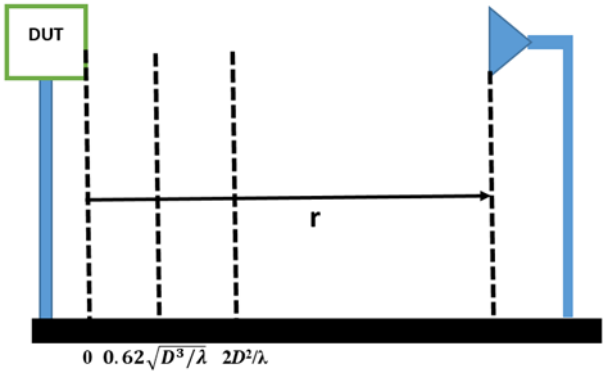

Fig. 3. OATS measurement setup

Mathematically, power received and normalized site attenuation (NSA) are expressed as [14]:

$$P_r = P_d A_e = \frac{E^2}{120\pi}\frac{\lambda^2 G_r}{4\pi} \quad (1)$$

$$NSA = \frac{279.1}{f E_{Max}} \quad (2)$$

where:
P_r is received power
P_d is power density
A_e is effective apperture
E is electric field strength
λ is wavelength
G_r is receiver gain
E_{Max} is maximum electric field strength
f is frequency

OATS is suitable to be used for measuring emissions for products with large sizes. According to [15], the maximum optimal distance is 30 m. Longer measuring distances will be very vulnerable to weather and radio noise in the vicinity, which can reduce the accuracy of the measurement. To obtain more accurate data, it is recommended that OATS is built in an area far from FM or TV transmitters or in an area with the worst FM and TV signals. If not, the technician must be able to distinguish between the signal from the DUT and the signal from another system (ambient signal) [15].

To overcome the influence of weather, structures with low reflection can be used. An example is a warehouse or site area cover. However, the effect of structure on accuracy needs to be examined. In [14], the time domain was used to separate the contribution of this structure.

Measurement accuracy using OATS is also determined by the equipment used, such as a test table and other support equipment [16]. Measurement uncertainty was discussed in more detail in [17]. According to research [17], there was a difference of 10 dB in results between a table with fiber glass material and wood. Also, there were a number of significant differences between the different woods. So, it should be recommended that the dielectric of the table material needs to be defined in the measurement standard using OATS. In addition to the table material, the table position also affects the emission measurement results [18]. It is then also recommended that the position of the test table should be included in the standard.

The OATS quality is determined by several factors, such as the construction of antenna elements, power supply, electrical properties, and sources of environmental scattering [19]. However, in OATS technique, interference frequently occurs from other sources [20]. To get a valid result, the interference must be eliminated or cancelled [20]. The proposed technique is a multichannel signal from an interference source and the equipment under test (EUT) being captured simultaneously on different antenna ports. A continuous stream of signals are sampled with very high speed sampling before being fed to the adaptive filter.

One of the applications of OATS is to measure the shielding effectiveness of connectors and coaxial cables as described in [21]. In that study [21], the working frequency was in the range of 200 MHz to 2 GHz and the study was situated in the open area of Farm Brazil between the mountains. The measurement results on OATS were compared with simulations using CST. Also, OATS is commonly used for EMC air craft certification tests as it has a very large space [22]. Table 2 presents several studies and applications of OATS.

Table 2. Studies and applications of OATS technique

References	Studies and Applications
[21]	Measurements of shielding effectiveness of connectors and coaxial cable
[22]	Testing for high intensity radiated field of unmanned aerial vehicle's
[23]	EM Emission from handheld devices
[20]	Cancellation of interference for emission measurement in OATS
[24]	Measurements of high level radiated susceptibility at the OATS
[25]	Modeling and correlation of radiated emissions generated at an OATS
[26]	Scattering characteristic analysis of OATS ground plane
[27]	Conversion of radiated emissions using genetic algorithm from anechoic chamber to OATS
[17]	Influences of table material at OATS on the strength of radiated field measurement
[28]	The diode loaded standard antenna as receiving in OATS
[29]	Ultra-broadband calculable dipole antennas verification & applications
[30]	Measuring radiated EMI using a statistical based model in OATS environment
[31]	Technique to compute OATS uncertainty
[32]	Model of GTD for OATS with a finite metallic plane

3.2. Anechoic Chamber

Anechoic chamber is a room covered by radiation absorbing material (RAM). There are two common absorbing materials, such as dielectric and ferrite absorber [33]. The dielectric absorber is used for the measurement of EM waves at GHz frequencies, while the ferrite absorber is used for the lower frequencies [34]. The main reason for using anechoic chamber as EM emission testing is because it is an ideal space for emission measurement without any effects from outside interference and weather [34].

Absorbent engineering is the key to chamber performance. To work properly, the depth of the cone on the absorber is proportional to the wavelength or greater [16]. The

performance decreases when the absorber depth is smaller than the wavelength. Therefore, it requires an absorber with a larger size. However, this implementation will be very expensive and require many spaces. Mechanically, it is also difficult to install and maintain.

To optimize the design, the performance of the absorbent shape has been simulated analytically [35]. Analytical homogenization for low-frequency absorbers was presented by Kuester [36]. With carbon coating, the performance of conical absorbers can be improved [37]. Ferrite tiles can be used for better absorption; however, it can only work on low bandwidth. To increase the bandwidth, several layers of ferrites are made [38]. To obtain an absorber for high bandwidth, it is necessary to combine it with a conical absorber [39]. To optimize this combination, numerical techniques can be used [40]. A better solution for future research is to use an active absorber that can be adjusted according to the type and frequency of work of the DUT [41].

Although being smaller compared to the absorber, reflections on the AC will interfere with antenna reception. Accurate results can be obtained by subtracting the reflection loss from the test results obtained. Loss of reflection (RL) is calculated as follows [42]:

$$Z_{in} = \sqrt{\frac{\mu_r}{\varepsilon_r}}.tanh\left(j\frac{2\pi fd}{c}.\sqrt{\mu_r\varepsilon_r}\right) \quad (3)$$

$$\rho_l = \frac{Z_{in} - Z_0}{Z_{in} + Z_0} \quad (4)$$

$$RL = -20\ log_{10}(\rho_l) \quad (5)$$

where:
Z_{in} is input impedance
μ_r is relative permeability of material
ε_r is relative permittivity of material
d is absorber thickness
f is frequency of radio wave
c is speed of light
ρ_l is reflection coefficient
Z_0 is 377 ohms

For the evaluation and diagnostics of reflections in the chamber, several methods have been developed. In [43] the use of a large waveguide and a coaxial line was presented. Meanwhile, [44] used the time domain to measure the absorber wall and [45] proposed the pencil matrix method to identify the relative strength of the direct and reflected path signals. The time domain approach is particularly useful in performing diagnostics in space because individual locations (e.g. walls, corners, or peripherals) can be isolated in time records and measured.

Figure 4 presents the anechoic chamber room at Universiti Kebangsaan Malaysia (UKM) Malaysia.

The test room of anechoic chamber is narrower than OATS. This chamber can provide a more controlled measurement compared to OATS because it is a closed room equipped with RAM (radiation absorbing material). This can help to prevent any external interference from affecting the measurement results. Similar to OATS, anechoic chambers are also good to evaluate far-field radiation patterns in shorter time directly.

An evaluation of measurement uncertainty in anechoic chamber is provided by CISPR 16-4-2 [46]. The results of the Site Voltage Standing Wave Ratio (SVSWR) of the chamber are used as the base for calculating the contribution of site-induced uncertainty. SVSWR data is then used to estimate the uncertainty of measurement from radiated emission results, called the Measurement Instrumentation Uncertainty (MIU) [46].

Fig. 4. AC room at microwave technology laboratory, UKM-Malaysia

Dina et.al used a semi anechoic chamber for emission testing of a laptop [47]. According to the IEC standard 61000-6-3, measurements are made at a distance of 3 meters. EMI radiation from the laptop was assessed in the frequency domain with a frequency of 30 MHz to 1 GHz, compliant with the CISPR 22 Standard.

Hofmann et.al studied the effect of broad electrical structure on the EMC-compliance of a semi-anechoic chamber [34]. A semi-anechoic chamber was used for evaluating the impact of large and permanently mounted objects on the propagation conditions [48]. Table 3 presents several studies and applications of AC.

Table 3. Studies and applications of AC technique

References	Studies and Applications
[44]	Characterizing the reflection coefficient of RAM using time domain technique
[45]	Evaluation of AC using matrix pencil technique
[46]	Contributions of site for radiated emission measurement Uncertainties more than 1 GHz
[47]	Laptop emission
[48]	Effect of electrically large structures on the EMC compliance
[49]	Single probe anechoic chamber technique for MIMO OTA measurement
[50]	Radiation pattern measurement for modulated metasurface antenna
[51]	Radiation pattern measurement for wideband low-sidelobe short array antenna
[52]	Radiation pattern measurement for arbitrary phased array system
[53]	Testing the effectiveness of the shared tower scale model
[54]	Radiation pattern measurement for monopole antenna with the periodic patch director
[55]	Validation of connector emission measurement
[56]	Simulations of automotive EMC
[57]	Effect of table material on radiated immunity Test
[58]	Radiated emissions measurement from an automotive cluster

3.3. CATR

The CATR technique was invented by Ricard Johnson and Poinsett of the Georgia Institute of Technology in 1966 [59]. This technique is used to measure EM emissions, mainly Radar Cross Section (RCS) [60]. The principle of CATR is to convert spherical waves to plane waves using a parabolic reflector [60]. Figure 5 shows the illustration of measurement setup of CATR.

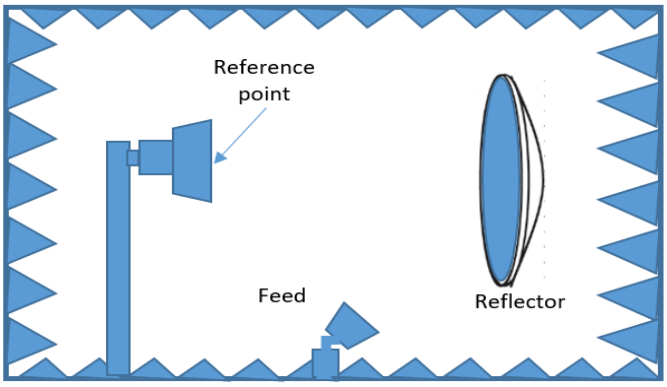

Fig. 5. Illustration of measurement setup of CATR

The feed position or DUT must be correct so that the direction of transmission by the source is right into the parabolic reflector. This will make the electromagnetic waves transmitted by the source well received by the receiver/DUT. If the feed position or DUT is incorrect, it can lead to direct interaction with the DUT [61].

Factors that affect the accuracy of antenna measurements on CATR have been identified by McCormics et.al [62]. The sources of antenna measurement errors include the alignment of AUT, multi-path, test zone quality, RF path dynamic/static variation, RF system linearity, RF system dynamic range, leakage and cross talk, channel imbalance, system drift, and random errors [62].

The determination of the mirror surface in CATR is very challenging due to the high requirements of the far-field properties of the antenna system. Surface accuracy checks are the easiest way to prove far-field characteristics. Laser tracking can be used for testing surface accuracy and alignment on CATR. In a study conducted by M. Juretzko and E. Richter, the tracking laser was able to accurately determine the CATR reflector. The measurement error using this technique is about 0.02 and provides satisfaction up to a frequency of 100 GHz. Operational techniques using a deeper laser can be read in [63]. This is a main issue, so it can cause diffraction from the fringer of the reflector, which results in a non-identical field. The use of a tri-reflector system has been used to improve CATR performance [61][64]. Table 4 presents studies and applications using CATR technique.

3.4. TEM Cell

The TEM cells are another technique for measuring electromagnetic fields apart from OATS and chambers. OATS and chamber techniques are very dependent on the antenna, so that the performance of the measurement is determined by the limitations of the antenna. However, TEM cells avoid the dependence on external or additional antennas as a part of the measurement system to measure EM radiation. Figure 6 shows the close and open TEM cell structure. TEM cells consist of a rectangular transmission line, the ends of which are taped with a standard coaxial connector. To avoid interference from outside, the close TEM cell is covered with a shield. However, the limitation of TEM cell is that the system frequency is limited by the dimensions of the TEM cell even though the TEM cell dimensions also have an effect on the dimensions of the DUT as a measurement object.

Table 4. Studies and applications of CATR Technique

References	Studies and Applications
[59]	Techniques employing CATR
[62]	Impact of measurement accuracy on CATR for high power testing
[63]	Calibration and alignment for CATR
[65]	Feed scanning using APC technique for CATR
[66]	The technique of antenna measurement uncertainty in CATR
[67]	Portable CATR for 5G using reflectarray
[68]	Ultra-Wideband Antennas measurement in a CATR
[69]	A New CATR for testing EW-Antenna
[70]	A 1.5-m Reflector Antenna testing at 322 GHz in a CATR based on a Hologram
[71]	The Odin Telescope at 119 GHz measurement using CATR (Hologram)
[72]	650 GHz antenna Test using CATR
[73]	Characterization of quit zone in mm-wave CATR
[74]	CATR using small F/D transmitarray
[75]	Genetic Evolution for optimization Blended Rolled Edge of a Rectangular Single Offset-Fed CATR
[76]	CATR feed using conical horn in mm bands

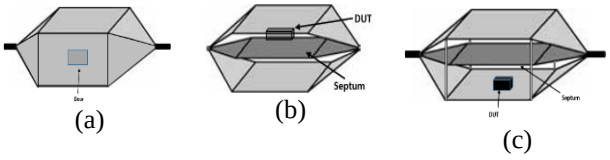

Fig. 6. TEM cell structure (a) close TEM cell (b) Inside of close TEM cell (c) Open TEM cell

The EM wave propagating in a TEM cell has an impedance of 377 ohms. This impedance is equal to the impedance of the wave in a free space. The impedance value of 377 ohms describes the relationship between the magnetic field amplitude (A/m) and the electric field amplitude (V/m). Due to this free space impedance, the magnetic field measurement of the DUT is uniform.

The characteristic impedance of TEM cell can be expressed as [77]:

$$Z_0 = \frac{1}{vC_0} = \frac{1}{\frac{1}{\sqrt{\mu_0 \varepsilon_0}} C_0} = \frac{\eta_0 \varepsilon_0}{C_0} \quad (6)$$

where:
Z_o is impedance
$\eta_o = 120\pi$ ohm is intrinsic impedance of free space
$\varepsilon_o = 8.854 \times 10^{-12}$ F/m is permitifity of free space
$\mu_o = 4\pi \times 10^{-7}$ H/m is permeability of free space
$v = 3 \times 10^8 m/s$
C_o is capacitance per unit length

The performance of TEM cells decrease due to the impedance mismatch of the septum so that the VSWR increase.

The method to solve this problem is by finding the connection point between the transmitting part of the septum and the main part. Several methods of septum have been designed without changing the cell size. Hence, the distribution of electric and magnetic fields is perfect. More details on cell septum design can be found in [78]. This septum redesign can reduce VSWR from 1.38 to 1.20 [78]. There is a variation of error in emission measurement from IC due to different environment and laboratory equipment [79].

Figure 7 illustrates the interconnection of the system components for measurement using TEM cell.

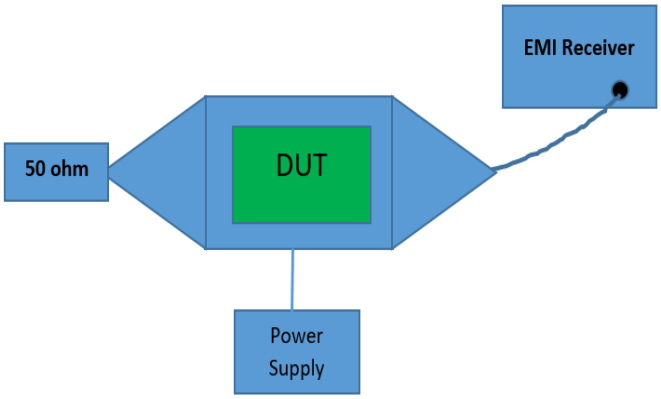

Fig. 7. Interconnection in TEM cell system

There are two types of TEM cell, namely closed TEM cell and open TEM cell as presented in Figure 6. The concept of closed TEM cell is as described above. In general, the advantage of open TEM cell is that it is easier to control the DUT function [80]. In more detail, its advantages of open TEM cell include the low cost, light weight and easy to store. Moreover, it can be used for DUT with larger and longer size. While the disadvantage of open TEM cell is that it is susceptible to ambient noise. In the case of closed TEM cells, the overall noise from outside is reduced but the size of the DUT is limited according to the size of the cell door [81].

The procedure for measuring the EMC of an IC follows the standard of IEC 61967-2 [82]. The septum is an inner conductor with a characteristic impedance of 50 ohms. Radiation characteristics can be seen in the spectrum analyzer.

An important aspect in TEM cells is the mode of propagation. The study of the effect of the propagation mode on radiated immunity has been carried out by Koohestani et al. [83]. That paper presented the reality that TEM cell manufacturers often provided cells with frequencies outside the dominant frequency. From that study, it was decided that cells can be employed at a higher frequency unlike the recommendation from IEC 61967-2 which must use TEM cells under the dominant mode frequency. Also, the location of the DUT within the TEM cell should be considered to assess proper immunity. That study recommended that immune testing be carried out using an open TEM cell because it is easier to move the position of the DUT [83].

In addition to VSWR, field polarization also affects the characterization of radiation emission in TEM cells. A comprehensive study of the effect of this EM polarization can be found in [84]. In this study, LoRa and WiFi were used with the frequencies of 433 MHz and 2.4 GHz, respectively. These two antennas were placed in open TEM cells with different orientations. There were 16 case studies in this study including the polarization along the x, along the y-axis, Position 5mm below the septum, the polarization along the x and y, and the polarization along the z. A more complete scenario can be read in [84]. The findings of the study showed that the power level was dependent not only on the orientation of the antenna, but also on the position of the antenna. Also an important finding was related to the determination of the cut-off frequency not only from the VSWR value as issued by the manufacturer, but also the cell dominant mode and field polarization [84]. Table 5 presents the studies and application using TEM Cell.

Table 5. Studies and application of TEM cell technique

References	Studies and Applications
[78]	The Optimization Design of Septum in TEM Cells for IC EMC Measurement
[79]	IC Radiated Emission (test and error analysis)
[80]	Development and test analysis of open TEM cell
[85]	Strip-line TEM cell for EMC Test
[86]	TEM cell for radiation and immunity measurement of transmission line
[87]	TEM cell improvement for testing IC
[88]	E-field measurement in the GSM frequency using E-probe in the TEM Cell
[89]	Analysis of emission sources from IC using rotating test board technique in TEM cell
[90]	Model of coupling determination of common mode chokes using TEM cell
[91]	Evaluation of electric and magnetic field shielding board level shield can using TEM cell
[92]	A New RLC structure measurement technique employing TEM cell
[93]	Design of TEM cell to test the electromagnetic sensor
[94]	Characterize Electric and Magnetic Field Coupling
[95]	Analysis of E-field of IC
[96]	an Interlaboratory Comparison of Radiated Emission
[97]	Performance investigation for 0.08 GHz to 6 GHz frequency of the GTEM.
[98]	Measurements of radiated emissions of a portable power bank in a GTEM cell
[99]	Measurement of EMC using GTEM Cell

3.5. RC

RC is frequently used for EMC testing as it provides a large area and is cheaper than other techniques with large space such as OATS and AC [100]. The RC does not require RF absorption material on the walls. The electromagnetic waves in the RC are reflected many times, which represents a multipath process [101].

When using the RC as an emission test, the antenna is positioned as the receiver, while the DUT is the transmitter. The emission characteristics of the DUT are analyzed from the results recorded by the receiving antenna. Figure 8 illustrates the measurement setup of RC and Figure 9 shows the example of RC room [102].

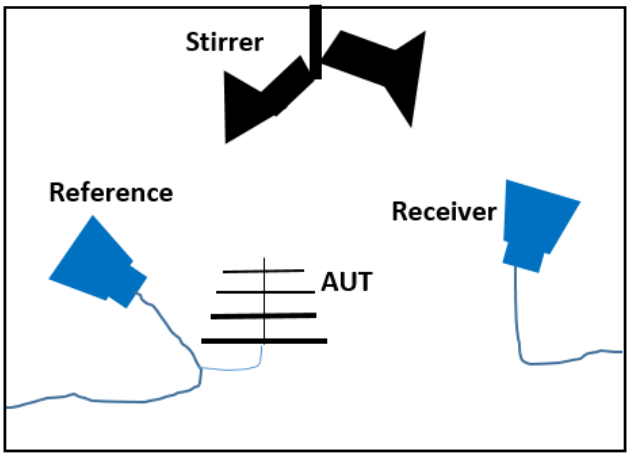

Fig. 8. Measurement setup of RC

Fig. 9. RC room [102] (Permission to reuse the figure granted by IEEE. License Number: 5356950061902)

Mathematically, the transmitted power, received power, and reflected power of the chamber walls and paddles are expressed as [103]:

$$P_T = \eta_A^{Total} P_{i1} \quad (7)$$

$$P_R = \eta_B^{Total} P_{o2} \quad (8)$$

$$P_{rf} = \eta_A^{Total} P_{o1} \quad (9)$$

where:
P_T is the transmitted power in the chamber
P_R is the average of received power
P_{rf} is the reflected energy of the chamber walls
η_A^{Total} is the total effciency of antenna port 1
η_B^{Total} is the total effciency of antenna port 2
P_{i1} is the input power to the antenna port 1
P_{o2} is the output power of antenna port 2
P_{o1} is the output power of antenna port 1

The RC is especially suitable for wireless applications because it models a multipath environment, simulating plane waves arriving from various angles and polarizations making it suitable for cell phone antenna testing [104]. With the development of wireless devices, the study of testing wireless devices in RC is a promising research. Table 6 presents studies and applications using RC technique.

3.6. NFS

Another technique for measuring EM emissions is by near field scanning. This technique does not require a large space like OATS and anechoic. One of the applications of the NFS is to provide near field data for the far-field prediction of a DUT [136]. Besides, it has been proven for antenna design tests and for measuring PCB and IC emission for EMC analysis [137] [138][139][140][141]. Figure 10 shows the near-field measurement operation mode. DUT is placed on the test table, the probe moves to perform scanning measuring the near-field of the PCB. In addition to measuring emissions, near-field measurements can also be used for immunity measurement [142]. In NFS technique, scanning is commonly performed near the PCB at many points, so that the source of emission problem can be easily detected (source localization).

Table 6. Studies and application of RC technique

References	Studies and Applications
[105]	Implemented Algorithm Characterization for MIMO Spatial Multiplexing in RC
[106]	Antenna efficiency measurement in a RC
[107]	Independent samples number investigation and the measurement uncertainty in a RC
[108]	EMC Applications for Military: RC Tests
[109]	Stirrer design optimization in a RC
[110]	Vehicle wideband wireless channels modelling using RC theory
[111]	Emission in RC: Numerical Evaluation of the total power radiated
[112]	The influence of stirrers using FDTD analysis in a RC
[113]	Cell tissue exposure tests using RC
[114]	Propagation studies for urban using RC
[115]	Pattern of antenna radiation measurements in RC
[116]	Power delay measurement in wireless environment using RC
[117]	Multipath channel simulation for BER measurement using RC
[118]	Material reflectivity and absorption measurement using RC
[119]	Measurement of Emission using RC for small DUT
[120]	IC immunity testing in RC
[121][122]	Spatial correlation functions of fields in a RC
[123]	Measurements of shielding effectiveness of materials using nested RC
[124]	Radiated Power Measurements in Reverberation Chambers
[125]	Antenna efficiency measurement in RC
[126]	Total radiated power measurement in uncalibrated RC
[127]	Statistical uncertainty simulation of emission measurements in an ideal RC
[104]	Isotropic and fading sensitivity using CDMA Phones in RC
[128]	Increased power and compensation when OTA testing of BS in LTE systems using RC
[129]	Model of exponential correlation for intensity of electric field
[130]	Stirred mode RC for radio type approval emission measurements
[131]	Shielding Effectiveness measurement of Sparsely Mode Enclosures in a RC
[132]	Around power density and electric field from broadband wireless emissions in a RC
[133]	Vehicle emission measurement using RC
[134]	Improved technique for reconstruction antenna pattern in a RC
[135]	Estimation of antenna gain pattern in a RC

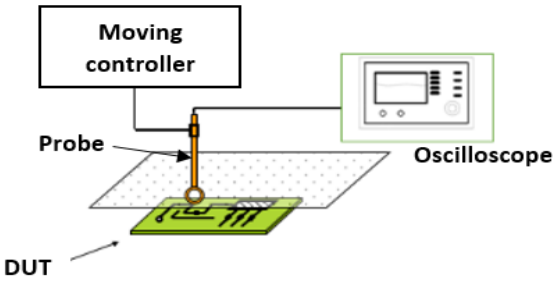

Fig. 10. Near-field measurement schematic

In near-field scanning technique, the choice of probe is an important factor. Based on IEEE standard, the loop antenna and monopole antenna have a good performance [143]. The calibration of the probe is essential to increase the validity of near-field measurements. The probe that requires calibration is the H (magnetic field) probe. H probes use loop antenna, and often sensitive to E (electric field). Ideally, the H probe is insensitive to electric fields. Figure 11 shows the E-Probe and H-Probe at the Near-Field Laboratory-UKM Malaysia. These probes are manufactured by Langer EMV-Technik [144]. Mathematically, the outputs of the electric and magnetic probes are expressed as [145] [146]:

$$i = CA\frac{dE(t)}{dt} \tag{10}$$

$$V_{emf} = -\frac{d\phi}{dt} = -\frac{d}{dt}\iint_s B.ds \tag{11}$$

where:
i is electric current
C is capacitance
A is system constant
$E(t)$ is Electric field
V_{emf} is EMF voltage
ϕ is magnetic flux
B is magnetic flux density

(a)

(b)

Fig. 11. (a) E-probe and (b) H-probe at near-field lab-UKM Malaysia

The electromagnetic characterization of IC using near-field scanning has been carried out by Harwot [147]. In this study, one magnetic probe was used. The DUT used was an FPGA with two operating modes, namely running-halted processor and DDR read-write. That study focus on the FPGA Emission characterization when running processor, halted processor mode, and DDR read-write operating modes. There are different levels of EM emission in different modes.

The near-field scanning technique on PCB with a 6-port approach has been carried out by Fengchao et.al [148]. The DUT used was a microstripline (MSL). That study has conclusion that EM emission result of 6 port approach agrees with emission measurements using VNA.

The emission characterization study on complex electronic products has been carried out by Hafiz [149]. The stochastic nature of electromagnetic emission is a challenge for the characterization process. Hafiz et.al developed an efficient field-field correlation measurement strategy as well as an efficient numerical technique to model the propagation of emission transients. The numerical approach used was the Wigner Distribution Function (WDF) approach, which required field-field correlation function (CF) as an input. The CF could be obtained by performing NFS on a plane with a size of 30 cm x 30 cm above a DUT. The DUT providing the stochastic radiated fields consisted of a metallic rectangular box with a field mixing mechanical stirrer and a monopole antenna mounted on the wall inside the enclosure. In this work, the input data would be the NFS measurement data at 1 cm, which was to be propagated to 5 and 10 cm using the WDF based propagation algorithm. Figure 12 and figure 13 present the correlation function (CF) of stochastic emissions at a distance of 5 cm and 10 cm from the DUT respectively. Figure 12 (a) and 13 (a) are produced from the measurement data on a plane with the height of 5 and 10 cm respectively while Figure 12 (b) and 13 (b) are the approximated CF propagated by the algorithm to 5 and 10 cm respectively. Figure 12 and Figure 13 show a good agreement between prediction and measurement at the two altitudes. Thus, this technique shows that the integration of the propagation algorithm and NFS data works well for random source characterization.

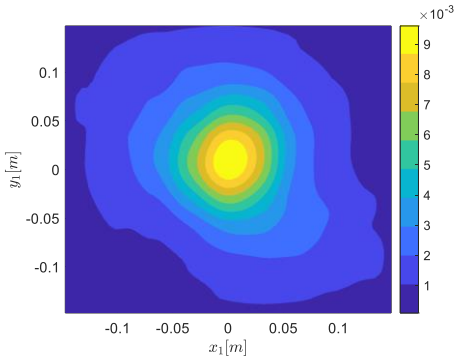

(a)

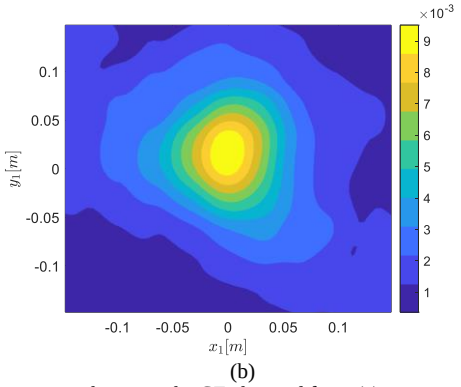

(b)

Fig. 12. Comparison between the CF obtained form (a) measured data and (b) approximate using propagators at distance of 5 CM

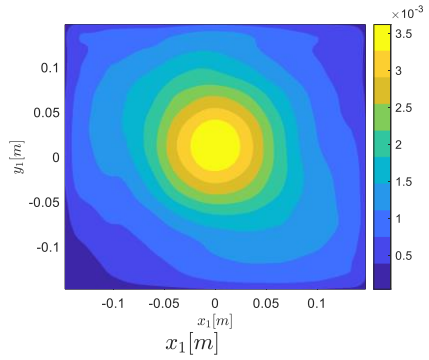

(a)

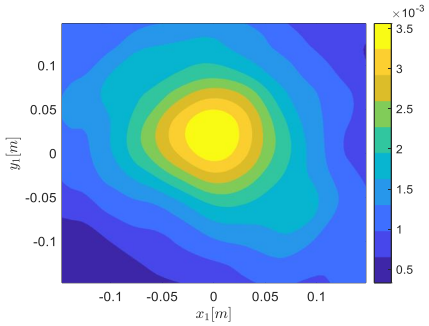

(b)

Fig. 13. Comparison between the CF obtained form (a) measured data and (b) approximate using propagators at distance of 10 CM

Table 7 presents other studies and applications of NFS.

4. Discussion

The techniques for measuring electromagnetic emissions has been described in Section 3. Each measurement technique has its own advantages and disadvantages. Hence, the technique needs to be chosen based on several considerations.

Based on space available for the test, the OATS technique has a very large space. The anechoic chamber has a narrower space than OATS. While reverberation chamber, CATR, TEM cell and NFS have small space. Next thing to consider is to look at the positioning error of DUT during the measurement. OATS, anechoic chamber, CATR, and TEM have low DUT positioning errors. The DUT positioning in the OATS is used to measure emission for the different orientations of the DUT. Thus, the DUT positioning error in the OATS is a source of inconsistency and error in ensuring that the strongest DUT emissions have been measured. In the CATR technique, the positioning error of the DUT will cause diffraction from the reflector edge because the field is not uniform. This is due to the direct interaction of the DUT with the antenna. In TEM, DUT positioning is used to assess multiple orientations. However, TEM cannot be operated while the DUT positioning is in upside down condition. The other techniques such as RC and NFS have very low positioning error. The NFS technique does not need the motion of the DUT for using a moving probe to scan for EM emissions.

In addition, OATS has the highest setup cost, while NFS has the lowest one. Comparing the complexity and experimental time of the emission measurement techniques, OATS and anechoic chamber have low usage complexity. The OATS and anechoic techniques do not require any complicated settings but this technique only requires a transmitter or receiver antenna dependent upon the purpose of the EM measurement. If it is to measure DUT emissions, then the antenna is used as a receiver. On the other hand, if it is to measure the immunity of the DUT, then the antenna is used as transmitter. Meanwhile, CATR, reverberation chamber, and near-field scanning have high usage complexity.

Table 7. Studies and application of NFS technique

References	Studies and Applications
[136]	Far-field estimation from efficient Near-field measurement
[138]	Current scan technique for the radiated emissions prediction of automotive systems based CISPR 25 standard
[139]	Degrading radiated emissions using near-field scan method for Automotive EMC
[140]	Near-field emissions analysis based on EBG structures From CM Filters
[142]	Radiated immunity of PCBs using near-field scanning
[150]	RF interference analysis using near-field shielding measurement in metallic mobile devices
[151]	Application of RFI for inverse MoM for source reconstruction in near-field scanning technique
[152]	3-D source reconstruction for near-field accuracy
[153]	Performances of near-field shielding of EMI noise suppression absorbers
[154]	Predicting far-fields from near-fields for EMC applications in broadband
[155]	Prediction the far-field using near-field scanning for microstrip line
[156]	Model of time-domain magnetic dipole of PCB Near-Field Emission
[157]	The minimum requirements model addressing the strength of electric and magnetic field strength measurement for use in near-field occupational exposure
[158]	Characterization of near-field for 13.56 MHz RFID
[159]	Near-field emission analysis from the PCB of a car deck player
[160]	The EM-Field probing Development for near-field scanning
[161]	SNR Optimization for low near-field scanning
[162]	Quick antenna examining using lowered near-field sampling
[163]	Characterization using near-field scanning
[164]	Near-field scan for investigating simultaneous switching noise

OATS, Anechoic chamber, RC, and CATR have small experimental time, in contrast to NFS. While TEM has the medium experimental time. For far-field emission, measurements directly using an OATS or anechoic chamber is recommended. This is because both have large space that can fit larger object and their complexity are very low as well. For the measurement of EM emissions on electronic products, it is recommended to use NFS. Besides being more economical, the source of emissions from electronic components can also be found. This cannot be achieved by using OATS and anechoic

chamber. Although NFS has some advantages, it still requires longer time consumption due to many measurement points and the post processing of the measurement data. For this, in implementing this technique, it is important to identify sufficient measurement data needed and to find an efficient and accurate post-processing technique.

Another challenge in EM emissions measurement is in performing it to complex electronic products. In this product, EMI is difficult to detect because it is non-stationary where it appears only at a certain frequency and time. This non-stationary characteristic can be due to the program running on board. The detection algorithm for this type of emission needs further attention and study so that electronic products are completely clean from EMI, which can exceed EMC standards. Table 8 presents the summary of emission measurement techniques.

Table 8. Summary of emission measurement techniques performance

Measurement techniques	Testing area	Complexity utilization	DUT positioning	Installation cost	Time consumption
OATS	Very wide	Very Low	Low	Very Expensive	Very low
AC	wide	Low	Low	Expensive	Very low
CATR	Small	Very high	Very low	Middle	Low
TEM Cell	Very small	Low	Low	Cheap	Low
RC	Small	High	Low	Cheap	Middle
NFS	Small	High	Very low	Very cheap	High

One of the challenges of EM emission analysis in electronic products is related to the emergence of non-stationary emission signals as discussed in [165]–[167]. Figure 14 shows the phenomenon of non-stationary emission from the Galileo operation [168]. The time domain plot is obtained from the measurement consisting of magnetic field probe, digital oscilloscope and Intel Galileo. During the measurement, the Galileo was programmed to run two different programs, i.e. Program 1 (filling random numbers into random elements and LED blinking) and Program 2 (LED blinking). Figure 14 shows the time series recorded as a result of the Galileo running Program 1. The time series clearly shows that the non-stationary of the emission is not present when the Galileo is running Program 2.

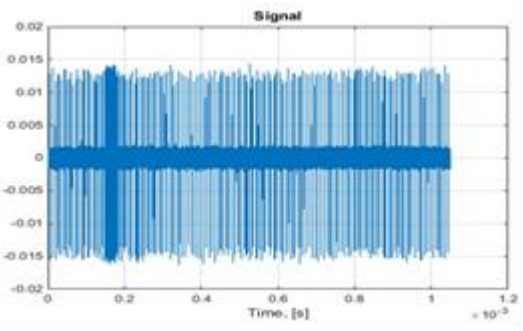

Fig. 14. Non stationary emission of Galileo operation [168] (Permission to reuse the figure granted by IEEE. License Number: 5356941408429)

The data that can be used as input to the propagation algorithm is the CF, which is calculated from stationary emissions source. As discussed in [169], the use of non-stationary series as input for methods designed for stationary series can lead to a misleading analysis.

One of the techniques to obtain stationary emission data from non-stationary emission data is by applying segmentation technique to achieve piecewise stationary. Several non-stationary analytical techniques have been discussed in [170][171] for speech processing and earthquake analysis. In [170][171] it showed that piecewise stationary time series could be generated from non-stationary time series segmentation.

Hafiz et.al proposed a method to achieve piecewise stationary from non-stationary emission signal by segmenting the non-stationary signal from figure 14 manually into 16 segments as shown in figure 15 [168].

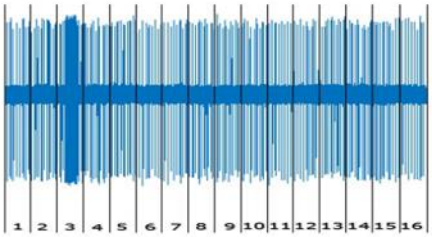

Fig. 15. Non-stationary EM emission time series divided by 16 segment manually [168] (Permission to reuse the figure granted by IEEE. License Number: 5356941408429)

The number of segments is fixed to focus more on the sorting technique being used. It can be clearly observed that two processes can be identified by running Program 1 above which are “filling random numbers into random elements” and “LED blinking processes”. 15 segments are produced while the LED is blinking and 1 segment while Galileo is believed to be doing the “filling random numbers into random elements”. This method is proven to be able to sort the short time segments based on their stationary characteristics. However, manually specifying the number of segments might cause some high emission signals to split into two parts. Besides, manual segmentation is unsuitable for solving the real problems in the field that require fast and efficient computation. So, the challenge ahead is to develop automatic segmentation of stationary emission to get piecewise stationary so that it can be used as input for propagation algorithms to support EM emission analysis in electronic products.

5. Conclusion

The techniques for measuring EM emissions have been discussed in this paper. The principles, advantages and disadvantages have also been discussed. Some considerations in selecting suitable techniques include space, cost, time consumption, and complexity. To save costs, the NFS technique come to be the right choice, but it requires computational development effort for post-processing of the near-field data. Another problem is the emergence of non-stationary EM emission from complex electronic devices. The

development for non-stationary emission segmentation and detection automatically should be a concern for future research.

Acknowledgements

The authors would like to acknowledge the support from the Geran Galakan Penyelidik Muda UKM (GGPM-2020-005) and Geran Universiti Penyelidikan UKM (GUP-2019-021).

References

1. A. K. Mallick, *Electromagnetic Pollution and Its Management, Handbook of Green Engineering Technologies for Sustainable Smart Cities*, CRC Press, 2021.
2. N. D. Mehta, M. Haque, A, and A. P. Patel, *An Overview of an Esoteric Pollution EMI-EMC, IRE J*. 2(2019) 69–76.
3. N. V Kantartzis and T. D. Tsiboukis, *Modern EMC Analysis Techniques*, Morgan & Claypool Publishers, 2008.
4. S. Ibrahim, *A comprehensive review on intelligent surveillance systems*, Commun. Sci. Technol. 1(2016) 7–14.
5. K. Wiklundh and P. Stenumgaard, *EMC challenges for the era of massive Internet of Things*, IEEE Electromagn. Compat. Mag. 8(2019) 65–74.
6. A. Maddocks, *Electromagnetic Compatibility*, UK: Elsevier, 2003.
7. K. Wyatt and R. Jost, *EMC Pocket Guide*. Scitech, 2013.
8. M. I. Montrose, *EMC & The Printed Circuit Board*. IEEE Press, 1998.
9. D. Morgan, *A Handbook of EMC Testing and Measurement*. London: The Institution of Engineering and Technology, 1994.
10. Paul and Clayton R, *Introduction to Electromagnetic Compatibility*. John Wiley & Sons, Inc, 2006.
11. CISRP, *Information technology equipment - Radio disturbance characteristics - Limit and methods of measurement*. Belgium, 2006.
12. E. Alan, C. C. Keskin, G. Kiraz, U. S. Ceran, and U. Dogan, *Experimental Analysis of Radiated Emission Limits Regarding Test Facilities According to EN 55032, 2019 Fifth International Electromagnetic Compatibility Conference (EMC Turkiye), Kocaeli, Turkey, 2019, pp. 1–5.*
13. C. . Balanis, *Antenna Theory*. John Wiley & Sons, Inc, 2005.
14. S. Eser and L. Sevgi, *Open-Area Test Site (OATS) Calibration*, IEEE Antennas Propag. Mag. 52(2010) 204–212.
15. P. Mathur and S. Raman, *Electromagnetic Interference (EMI): Measurement and Reduction Techniques*, J. Electron. Mater. 49(2020) 2975–2998.
16. P. F. Wilson, *Advances in radiated EMC measurement techniques*, URSI Radio Sci. Bull., 2004(2004) 65–78.
17. C. Zombolas, *The effects of table material on radiated field strength measurement reproducibility at open area test sites, IEEE International Symposium on Electromagnetic Compatibility, 2001, pp. 260–264.*
18. P. A. Beeckman, *The influence of positioning tables on the results of radiated EMC measurements, IEEE Int. Symp. Electromagn. Compat., 2001, pp. 280–285*.
19. I. Barbary *et al., On the quality of a real open area test site, IEEE Int. Symp. Electromagn. Compat., 2015, pp. 1201–1206.*
20. F. G. Awan and A. Kiran, *Cancellation of Interference for Emission Measurement in Open Area Test Site*, Measurement. 111(2017) 183–196.
21. K. M. G. Santos, M. S. Novo, G. Fontgalland, M. B. Perotoni, and C. L. Andrade, *Shielding effectiveness measurements of coaxial cable and connectors using compact open area test site*, J. Microwaves, Optoelectron. Electromagn. Appl. 16 (2017) 997–1011.
22. S. F. Romero, P. L. Rodriguez, D. E. Bocanegra, D. P. Martinez, and M. A. Cancela, *Comparing Open Area Test Site and Resonant Chamber for Unmanned Aerial Vehicle's High-Intensity Radiated Field Testing*, IEEE Trans. Electromagn. Compat. 60(2018) 1704–1711.
23. H. Garbe, *How to Reproducibly Measure the Unintended EMEmission from Handheld Devices, 5th International Conference on Consumer Electronics Berlin (ICCE-Berlin), 2015, pp. 211–212.*
24. M. Hoijer and M. Backstrom, *How we confused the comparison between high level radiated susceptibility measurements in the reverberation chamber and at the open area test site, 2003 IEEE International Symposium on Electromagnetic Compatibility, 2003, pp. 1043–1046.*
25. Desheng Zhu and Keng Yin Chok, *Modeling and correlation of radiated emissions generated in a fully anechoic chamber and at an OATS, 1998 IEEE EMC Symposium. International Symposium on Electromagnetic Compatibility, 1998, pp. 147–152.*
26. D. Qiao, Z. Qi, H. Mingliang, and S. Dong-An, *Analysis of scattering property of open-area test site ground plane, General Assembly and Scientific Symposium, 2014, pp. 4–7.*
27. J. R. Regué, M. Ribó, and J. M. Garrell, *Radiated emissions conversion from anechoic environment to OATS using a hybrid genetic algorithm - Gradient method, IEEE International Symposium on Electromagnetic Compatibility, 2001, pp. 325–329.*
28. J. Park, G. Mun, D. Yu, B. Lee, and W. N. Kim, *Proposal of simple Reference Antenna Method for EMI antenna calibration, IEEE International Symposium on Electromagnetic Compatibility, 2011, pp. 90–95.*
29. D. Meng, *Verification of ultra-broadband calculable dipole antennas & applications, 12th International Conference on Electronic Measurement and Instruments, 2015, pp. 1490–1493.*
30. F. G. Awan, N. M. Sheikh, S. A. Qureshi, and A. Ali, *A generic model for the classification of Radiation emission data in electromagnetic compatibility measurement, 2008 IEEE Radio and Wireless Symposium, 2008, pp. 315–318.*
31. E. R. Heise and R. E. W. Heise, *A method to compute open area test site uncertainty using ANSI C63.4 normalized site attenuation measurement data, Proceedings of Symposium on Electromagnetic Compatibility, 1996, pp. 505–507.*
32. Chun Hsiung Chen and Han-Chang Hsieh, *A GTD model for open area test site with finite metallic plane, IEEE International Symposium on Electromagnetic Compatibility, 2003, pp. 119-122.*
33. L. H. Hemming, *Electromagnetic Anechoic Chambers*. Canada: IEEE Press, 2010.
34. Q. Xu and Y. Huang, *Anechoic and Reverberation Chambers*. Hoboken, NJ: John Wiley & Sons Ltd, 2019.
35. C. L. Holloway and E. F. Kuester, *Modeling semi-anechoic electromagnetic measurement chambers*, IEEE Trans. Electromagn. Compat. 38 (1996) 79–84.
36. E. F. Kuester, *A Low-Frequency Model for Wedge or Pyramid Absorber Arrays—II: Computed and Measured Results*, IEEE Trans. Electromagn. Compat. 36 (1994) 307–313.
37. T. Ellam, *Update on the design and synthesis of compact absorber for EMC chamber applications, IEEE Int. Symp. Electromagn. Compat., 1994, pp. 408–412.*
38. H. Komori and Y. K. Fellow, *Wide Band Electromagnetic Wave Absorber with Thin Magnetic Layers*, IEEE Trans. Broadcast. 40 (1994) 219–222.
39. C. L. Holloway, P. M. McKenna, R. A. Dalke, R. A. Perala, and C. L. Devor, *Time-domain modeling, characterization, and measurements of anechoic and semi-anechoic electromagnetic test chambers*, IEEE Trans. Electromagn. Compat. 44 (2002) 102–118.

40. F. L. Teixeira, *On aspects of the physical realizability of perfectly matched absorbers for electromagnetic waves*, Radio Sci. 38 (2003) 1–10.
41. L. R. Arnaut, *Adaptive control and optimization of electromagnetic radiation, attenuation, and scattering using self-adaptive material systems*, IEEE Trans. Antennas Propag. 51 (2003) 1530–1548.
42. S. Khadka, *Evaluation of Radio Anechoic Chamber*, M.Sc Thesis, Helsinki Metropolia University of Applied Sciences, 2017.
43. S. Takeya and K. Shimada, *New measurement method of RF absorber characteristics by large square coaxial line*, *International Symposium on Electromagnetic Compatibility, 1993, pp. 397–402.*
44. S. Tofani, A. Ondrejka, and M. Kanda, *A time-domain method for characterizing the reflection coefficient of absorbing materials from 30 to 1000 MHz*, IEEE Trans. Electromagn. Compat. 33 (1991), 234–240.
45. B. Fourestié, Z. Altman, and M. Kanda, *Anechoic chamber evaluation using the matrix pencil method*, IEEE Trans. Electromagn. Compat. 41 (1999) 169–174.
46. Z. Chen and Z. Xiong, *Site contributions for radiated emission measurement uncertainties above 1 GHz*, *2017 IEEE International Symposium on Electromagnetic Compatibility & Signal/Power Integrity (EMCSI), 2017, pp. 504–509.*
47. L.-A. Dina, P.-M. Nicolae, I. D. Smarandescu, and V. Voicu, *Considerations on radiated emission measurements for a Laptop in a semi-anechoic chamber*, *2017 International Conference on Electromechanical and Power Systems (SIELMEN), 2017, pp. 202–207.*
48. W. Hofmann, C. Bornkessel, and M. A. Hein, *Influence of Electrically Large Structures on the EMC-Compliance of a Semi-Anechoic Chamber*, *2018 IEEE MTT-S International Conference on Microwaves for Intelligent Mobility (ICMIM), 2018, pp. 1–4.*
49. Q. Zhang, T. H. Loh, W. Zhang, Y. Yang, Z. Huang, and F. Qin, *A Low-Cost and Efficient Single Probe Based MIMO OTA Measurement Method*, IEEE Trans. Instrum. Meas. 71(2022) 1–15.
50. A. M. Hakimi, A. Keivaan, H. Oraizi, and A. Amini, *Wide-Scanning Circularly Polarized Reflector-Based Modulated Metasurface Antenna Enabled by a Broadband Polarizer*, IEEE Trans. Antennas Propag. 70(2022) 84–96.
51. P. Liu, G. F. Pedersen, and S. Zhang, *Wideband Low-Sidelobe Slot Array Antenna With Compact Tapering Feeding Network for E-Band Wireless Communications*, IEEE Trans. Antennas Propag. 70(2022) 2676–2685.
52. R. H. Kenney, J. L. Salazar-Cerreno, and J. W. McDaniel, *Two-Dimensional Beam Pattern Synthesis for Phased Arrays With Arbitrary Element Geometry via Magnitude Least Squares Optimization*, IEEE J. Microwaves. 2(2022) 337–346.
53. Z. Tang, F. Yu, W. Rao, S. Lv, Y. Cui, and W. Wang, *Electromagnetic Field Tests in the Anechoic Chamber Based on the Shared Tower Scale Model*, *2022 IEEE 2nd International Conference on Power, Electronics and Computer Applications (ICPECA), 2022, pp. 150–153.*
54. S. Youn, D. Jang, N. K. Kong, and H. Choo, *Design of a Printed 5G Monopole Antenna With Periodic Patch Director on the Laminated Window Glass*, IEEE Antennas Wirel. Propag. Lett. 21(2022) 297–301.
55. Manisha and N. Sood, *Validation of anechoic chamber for radiated emission test*, *15th Int. Conf. Electromagn. Interf. Compat., 2018, pp. 1–4.*
56. V. S. Reddy and P. Kralicek, *Modeling of semi-anechoic chamber for use in automotive EMC simulations*, *IEEE MTT-S Int. Microw. RF Conf., 2015, pp. 77–80.*
57. H. Shida *et al.*, *Influence of test table materials on radiated immunity test: Report on investigation using a giant anechoic chamber*, *Asia-Pacific Symposium on Electromagnetic Compatibility (EMC/APEMC), 2018, pp. 572–577.*
58. A. M. Silaghi, C. Balan, E. Tolan, and A. De Sabata, *The influence of measurement setups in radiated emissions testing, 2017 14th Int. Conf. Eng. Mod. Electr. Syst., 2017, pp. 220–223.*
59. R. Johnson and R. Ponsett, *Compact Antenna Test Range Techiques*, Technical Report, Griffiss Air Force Base, New York, 1966.
60. D. Fasold, *Measurement Performance of Basic Compact Range Concepts*, *AMTA Europe Symposium, 2006, pp. 1–11.*
61. C. S. Obiekezie, E*xtended Equivalent Dipole Model for Radiated Emissions*, Ph.D Thesis, University of Nottingham, UK, 2016.
62. J. McCormick, J. Boyce, J. Sayers, and J. Murray, *The impact on measurement accuracy of specifying a compact antenna test range for high power testing*, *IET Semin. Dig., 2007, pp. 1–6.*
63. M. Juretzko and E. Richter, *Compact Range Calibration and Alignment*, *AMTA Europe Symposium, 2006, pp. 270–275.*
64. C. . Balanis, *Antenna Theory Analysis and Design*, Canda:John Wiley & Sons, Inc, 2015.
65. V. Viikari, J. Häkli, J. Ala-Laurinaho, J. Mallat, and A. V. Räisänen, *A feed scanning based APC technique for compact antenna test ranges*, IEEE Trans. Antennas Propag. 53(2005) 3160–3165.
66. S. Blalock and J. A. Fordham, *Antenna measurement uncertainty method for measurements in compact antenna test ranges*, *2016 10th European Conference on Antennas and Propagation (EuCAP), 2016, pp. 1–5.*
67. A. F. Vaquero, M. Arrebola, M. R. Pino, R. Florencio, and J. A. Encinar, *Demonstration of a Reflectarray with Near-field Amplitude and Phase Constraints as Compact Antenna Test Range Probe for 5G New Radio Devices*, IEEE Trans. Antennas Propag. 69(2021) 2715-2726.
68. M. Nel, J. Joubert, and J. W. Odendaal, *The measurement of complex antenna transfer functions for ultra-wideband antennas in a compact range [measurements corner]*, IEEE Antennas and Propagation Magazine. 56 (2014) 163–170.
69. B. Svensson *et al.*, *A new compact antenna test range for EW-antenna system production testing*, *2017 11th European Conference on Antennas and Propagation, 2017, pp. 2585–2589.*
70. J. Häkli *et al.*, *Testing of a 1.5-m reflector antenna at 322 GHz in a CATR based on a hologram*, IEEE Trans. Antennas Propag. 53 (2005) 3142–3150.
71. J. Ala-Laurinaho *et al.*, *Measurement of the Odin telescope at 119 GHz with a hologram-type CATR*, IEEE Trans. Antennas Propag. 49(2001) 1264–1270.
72. A. Karttunen *et al.*, *Antenna tests with a hologram-based CATR at 650 GHz*, IEEE Trans. Antennas Propag. 57(2009) 711–720.
73. Y. Chen, L. Zhu, Y. Yao, H. Ge, J. Yu, and X. Chen, *Unified Initial Preprocessing for Phaseless Characterization of Quiet Zone in Millimeter-wave Compact Antenna Test Range*, IEEE Antennas Wirel. Propag. Lett. 1225(2022) 1–5.
74. J. Tang *et al.*, *Compact Antenna Test Range Using Very Small F/D Transmitarray Based on Amplitude Modification and Phase Modulation*, IEEE Trans. Instrum. Meas. 71(2022) 1-14.
75. S. F. Gregson, M. Dirix, and R. Dubrovka, *Efficient Optimization of the Blended Rolled Edge of a Rectangular Single Offset-Fed Compact Antenna Test Range Reflector Using Genetic Evolution*, *2022 16th European Conference on Antennas and Propagation (EuCAP), 2022, pp. 1–5.*
76. S. Pivnenko, A. U. Zaman, and M. Ivashina, *Using a Conical Horn as Compact Antenna Test Range Feed in Millimetre Bands*, *2022 16th European Conference on Antennas and Propagation (EuCAP), 2022, pp. 01–05.*
77. M. Kanda and R. D. Orr, *Generation of Standard Electromagnetic Field in a TEM Cell*, Technical Note, US National Bureau of Standards, Washington, 1988.

78. S. Wen, J. Zhang, and Y. Lv, *The optimization design of septum in TEM cells for IC EMC Measurement, 2015 7th Asia-Pacific Conference on Environmental Electromagnetics (CEEM), 2015, pp. 250–253.*
79. Y. Li, J. Wu, H. Li, H. Zhang, H. Ma, and J. Wu, *Comparison test and error analysis of the TEM cell method in IC radiated emission, 2018 IEEE International Symposium on Electromagnetic Compatibility and 2018 IEEE Asia-Pacific Symposium on Electromagnetic Compatibility (EMC/APEMC), 2018, pp. 1208–1211.*
80. H. M. Pathak, S. Shah, and H. O. Mode, *Development and test analysis of Symmetric Open TEM cell*, J. Sci. Technol. Res. 2(2020) 90–97.
81. A. Eadie, *TEM Cell and GTEM Guide For Radiated Emissions & Radiated Immunity Pre-Compliance Testing, 2019. https://emcfastpass.com/tem-cell-guide.*
82. IEC, *IEC 61967-2 : 2005 Integrated circuits - Measurement of electromagnetic. 2005.*
83. M. Koohestani, M. Ramdani, and R. Perdriau, *Impact of Mode Propagation on Radiated Immunity Characterization in Commonly Used TEM Cells, EMC COMPO 2019 - 2019 12th International Workshop on the Electromagnetic Compatibility of Integrated Circuits, 2019, pp. 5–7.*
84. M. Koohestani, M. Ramdani, F. L. Lafon, A. A. Moreira, and R. Perdriau, *Impact of Field Polarization on Radiated Emission Characterization in an Open TEM Cell*, IEEE Trans. Instrum. Meas. 69(2020) 6595–6602.
85. L. Wen, G. Yalin, and L. Jin, *Three new strip-line TEM cells in EMC test, 2016 IEEE International Conference on Electronic Information and Communication Technology (ICEICT), 2016, pp. 497–500.*
86. C. Shi, C. Chai, Y. Yang, Z. Ma, L. Qiao, and X. Yu, *Characterization of electromagnetic field-transmission line coupling of radiated emission and immunity using TEM cell measurement*, Prog. Electromagn. Res. Lett. 64(2016) 65-71.
87. A. V. Demakov and M. E. Komnatnov, *Improved TEM-cell for EMC tests of integrated circuits, 2017 International Multi-Conference on Engineering, Computer and Information Sciences (SIBIRCON), 2017, pp. 399–402.*
88. N. Narang, S. K. Dubey, P. S. Negi, and V. N. Ojha, *Precise E-field measurement inside TEM cell at GSM frequencies using microstrip E-field probe, 2016 International Conference on Signal Processing and Communication (ICSC), 2016, pp. 126–129.*
89. W. Fang *et al.*, *Extracting the Electromagnetic Radiated Emission Source of an Integrated Circuit by Rotating the Test Board in a TEM Cell Measurement*, IEEE Trans. Electromagn. Compat. 61(2019) 833–841.
90. M. Stojanovic, F. Lafon, S. Op'T Land, R. Perdriau, and M. Ramdani, *Determination of Equivalent Coupling Surface of Passive Components Using the TEM Cell*, IEEE Trans. Electromagn. Compat. 60(2018) 298–309.
91. H. Jang, J. Lim, Y. Lee, H. Lee, and W. Nah, *Electric and magnetic field shielding evaluation of board level shield can using TEM cell, in 2015 IEEE Electrical Design of Advanced Packaging and Systems Symposium (EDAPS), 2015, pp. 201–204.*
92. Y. Bacher *et al.*, *A new RLC structure measurement method using a Transverse ElectroMagnetic cell, 2015 IEEE International Circuits and Systems Symposium (ICSySS), 2015, pp. 7–10.*
93. H. Sinaga and B. H. Sitorus, *Design of tem cell to test the electromagnetic sensor*, ARPN J. Eng. Appl. Sci. 12(2017) 3783–3788.
94. C. Shi *et al.*, *Using Termination Effect to Characterize Electric and Magnetic Field Coupling Between TEM Cell and Microstrip Line*, IEEE Trans. Electromagn. Compat. 57(2015) 1338–1344.
95. K. L. Chua and M. Z. Mohamed Jenu, *Improved accuracy of GTEM cell/SAC-correlated measurement of IC-radiated electric fields by a correction factor*, ARPN J. Eng. Appl. Sci. 10(2015) 8441–8444.
96. A. Raizer and M. P. Fonseca, *Using a GTEM cell in an interlaboratory comparison of radiated emission, 2017 IEEE 3rd Glob. Electromagn. Compat. Conf, 2017, pp. 1–4.*
97. A. Vie, B. Loader, and D. Bownds, *Investigation of the performance of the GTEM 1750 from 0.08 GHz to 6 GHz, IEEE Int. Symp. Electromagn. Compat., 2016, pp.245–250.*
98. B. Palczynska, *Radiated emissions measurements of a portable power bank in a GTEM cell, 17th IEEE Int. Conf. Environ. Electr. Eng., 2017, pp. 0–5.*
99. P. Elter, A. Sabo, T. Szakáll, and B. Kuljić, *EMC Measurement with GTEM Cell*, J. Appl. Tech. Educ. Sci. 9(2019) 112–128.
100. J.-I. Hong and C.-S. Huh, *Optiimization of strirrer with arious parameters in reverberation chamber*, Prog. Electromagn. Res. 104(2010) 15–30.
101. A. Kundu, B. Gupta, K. Patra, and A. I. Mallick, *Role of Reverberation Chamber in Wireless Testing and Measurement with Emphasis on Investigating Biological Effects, 2020 IEEE Calcutta Conference (CALCON), 2020, pp. 132–136.*
102. *D. Mandaris et al., Different Test Site Analysis of Radiated Field Measurements of a Complex EUT, 2019 International Symposium on Electromagnetic Compatibility - EMC EUROPE, 2019, pp. 674–679.*
103. C. L. Holloway, H. A. Shah, R. J. Pirkl, W. F. Young, D. A. Hill, and J. Ladbury, *Reverberation chamber techniques for determining the radiation and total efficiency of antennas*, IEEE Trans. Antennas Propag. 60(2012), 1758–1770.
104. C. Orlenius, P.-S. Kildal, and G. Poilasne, *Measurements of total isotropic sensitivity and average fading sensitivity of CDMA phones in reverberation chamber, 2005 IEEE Antennas and Propagation Society International Symposium, 2005, pp. 409–412.*
105. X. Chen, P. S. Kildal, and M. Gustafsson, *Characterization of implemented algorithm for MIMO Spatial multiplexing in reverberation chamber*, IEEE Trans. Antennas Propag. 61(2013) 4400–4404.
106. X. Chen, *On statistics of the measured antenna efficiency in a reverberation chamber, IEEE Trans. Antennas Propag.* 61(2013) 5417–5424.
107. X. Chen, *Experimental Investigation of the Number of Independent Samples and the Measurement Uncertainty in a Reverberation Chamber*, IEEE Trans. Electromagn. Compat. 55(2013) 816–824.
108. C. Choeysakul, F. Schlagenhaufer, P. Rattanakreep, and P. Hall, *EMC applications for military: Reverberation chamber tests, The 20th Asia-Pacific Conference on Communication (APCC2014), 2014, pp. 434–437.*
109. J. Clegg, A. C. Marvin, J. F. Dawson, and S. J. Porter, *Optimization of stirrer designs in a reverberation chamber*, IEEE Trans. Electromagn. Compat. 47(2005) 824–832.
110. O. Delangre, S. Van Roy, P. De Doncker, M. Lienard, and P. Degauque, *Modeling in-Vehicle Wideband Wireless Channels Using Reverberation Chamber Theory, 2007 IEEE 66th Vehicular Technology Conference, 2007, pp. 2149–2153.*
111. F. Diouf, F. Paladian, M. Fogli, C. Chauvière, and P. Bonnet, *Emission in reverberation chamber: Numerical evaluation of the total power radiated by a wire with a stochastic collocation method, Proceedings of the 18th International Zurich Symposium on Electromagnetic Compatibility, 2007, pp. 99–102.*
112. K. Harima and Y. Yamanaka, *FDTD analysis on the effect of stirrers in a reverberation chamber, 1999 International Symposium on Electromagnetic Compatibility, 1999, pp. 260–263.*
113. L. O. Fichte, K. Grutzat, and M. Stiemer, *On the use of electromagnetic reverberation chambers for exposiure tests of cell tissue, 2012 6th Asia-Pacific Conference on Environmental Electromagnetics (CEEM), 2012, pp. 329–332.*
114. H. Fielitz, K. A. Remley, C. L. Holloway, Q. Zhang, Q. Wu, and D. W.

Matolak, *Reverberation-chamber test environment for outdoor urban wireless propagation studies*, IEEE Antennas Wirel. Propag. Lett. 9(2010) 52–56.

115. M. A. Garcia-Fernandez, C. Decroze, and D. Carsenat, *Antenna radiation pattern measurements in reverberation chamber using Doppler analysis, Conference on Antenna Measurements & Applications (CAMA), 2014, pp. 1–4.*
116. E. Genender, C. L. Holloway, K. A. Remley, J. Ladbury, G. Koepke, and H. Garbe, *Use of reverberation chamber to simulate the power delay profile of a wireless environment, 2008 International Symposium on Electromagnetic Compatibility - EMC Europe, 2008, pp. 1–6.*
117. E. Genender, C. L. Holloway, K. A. Remley, J. M. Ladbury, G. Koepke, and H. Garbe, *Simulating the multipath channel with a reverberation chamber: Application to bit error rate measurements*, IEEE Trans. Electromagn. Compat. 52(2010) 766–777.
118. A. Gifuni, *On the Measurement of the Absorption Cross Section and Material Reflectivity in a Reverberation Chamber*, IEEE Trans. Electromagn. Compat., (2009) 1047–1050.
119. K. Harima, *Radiated emission measurement of small EUT by using a reverberation chamber, 2003 IEEE International Symposium on Electromagnetic Compatibility, 2003, pp. 471-474.*
120. R. Heinrich, R. Bechly, and B. Deutschmann, *Radiated immunity testing of integrated circuits in reverberation chambers, IEEE International Symposium on Electromagnetic Compatibility, 2012, pp. 8–11.*
121. D. A. Hill, *Spatial correlation function for fields in a reverberation chamber*, IEEE Trans. Electromagn. Compat. 37(1995) 138.
122. D. A. Hill and J. M. Ladbury, *Spatial-correlation functions of fields and energy density in a reverberation chamber*, IEEE Trans. Electromagn. Compat. 44(2002) 95–101.
123. C. L. Holloway, D. A. Hill, J. Ladbury, G. Koepke, and R. Garzia, *Shielding effectiveness measurements of materials using nested reverberation chambers*, IEEE Trans. Electromagn. Compat. 45(2003) 350–356.
124. G. Koepke and J. Ladbury, *Radiated Power Measurements in Reverberation Chambers, 56th ARFTG Conference Digest, 2000, pp. 1–7.*
125. H. G. Krauthauser and M. Herbrig, *Yet another antenna efficiency measurement method in reverberation chambers, 2010 IEEE International Symposium on Electromagnetic Compatibility, 2010, pp. 536–540.*
126. H. G. Krauthauser, *On the Measurement of Total Radiated Power in Uncalibrated Reverberation Chambers*, IEEE Transactions on Electromagnetic Compatibility, 49(2007) 270-278.
127. M. Magdowski and R. Vick, *Monte Carlo simulation of the statistical uncertainty of emission measurements in an ideal reverberation chamber, International Symposium on Electromagnetic Compatibility, 2017, pp. 1–6.*
128. D. Micheli, M. Barazzetta, F. Moglie, and V. M. Primiani, *Power Boosting and Compensation During OTA Testing of a Real 4G LTE Base Station in Reverberation Chamber*, IEEE Trans. Electromagn. Compat. 57(2015) 623–634.
129. C. Carobbi and R. Serra, *Exponential correlation model for electric field intensity in reverberation chambers, 16th European Conference on Antennas and Propagation (EuCAP), 2022, pp. 1–5.*
130. J. Page, *Stirred mode reverberation chambers for radio type approval emission measurements, IEE Colloquium on EMC Tests in Screened Rooms, 1995, pp. 1–11.*
131. G. B. Tait, C. Hager, M. B. Slocum, and M. O. Hatfield, *On Measuring Shielding Effectiveness of Sparsely Moded Enclosures in a Reverberation Chamber*, IEEE Trans. Electromagn. Compat. 55(2013) 231–240.
132. G. B. Tait, C. E. Hager, T. T. Baseler, and M. B. Slocum, *Ambient Power Density and Electric Field From Broadband Wireless Emissions in a Reverberant Space*, IEEE Trans. Electromagn. Compat. 58(2016) 307–313.
133. R. Wen, *Using reverberation chamber for vehicle radiated emission measurement, 2015 Asia-Pacific Symposium on Electromagnetic Compatibility (APEMC), 2015, pp. 75–77.*
134. J. Zheng, X. Chen, X. Liu, M. Zhang, B. Liu, and Y. Huang, *An Improved Method for Reconstructing Antenna Radiation Pattern in a Loaded Reverberation Chamber*, IEEE Trans. Instrum. Meas. 71(2022) 1-12.
135. A. Reis, F. Sarrazin, P. Besnier, P. Pouliguen, and E. Richalot, *Contactless Antenna Gain Pattern Estimation from Backscattering Coefficient Measurement Performed Within a Reverberation Chamber*, IEEE Trans. Antennas Propag. 70(2022), 2318–2321
136. Ding Yu, Gang Jiang, Lin Yang, and Demin Fu, *An efficient near-field measurement technique for predicting far-field monostatic RCS of targets, 2015 IEEE 6th International Symposium on Microwave, Antenna, Propagation, and EMC Technologies (MAPE), 2015, pp. 189–192.*
137. A. Boyer, N. Nolhier, F. Caignet, and S. Ben Dhia, *On the Correlation Between Near-Field Scan Immunity and Radiated Immunity at Printed Circuit Board Level – Part II*, IEEE Trans. Electromagn. Compat. (2022)1–13.
138. J. Jia, D. Rinas, and S. Frei, *Predicting the Radiated Emissions of Automotive Systems According to CISPR 25 Using Current Scan Methods*, IEEE Trans. Electromagn. Compat. 58(2016) 409–418.
139. A.-M. Silaghi, R.-A. Aipu, A. De Sabata, and P.-M. Nicolae, *Near-field scan technique for reducing radiated emissions in automotive EMC, 2018 IEEE International Symposium on Electromagnetic Compatibility and 2018 IEEE Asia-Pacific Symposium on Electromagnetic Compatibility (EMC/APEMC), 2018, pp. 831–836.*
140. C. Olivieri *et al.*, *Analysis of Near-Field Emissions From Common-Mode Filters Based on EBG Structures*, IEEE Trans. Electromagn. Compat. 59(2017) 593–599.
141. G. Langer and J. Hacker, *Determining the Emission of a Device from the Near Field of an IC, 12th International Workshop on the Electromagnetic Compatibility of Integrated Circuits, 2019, pp. 67–69.*
142. A.Durier, S. Ben Dhia, and T. Dubois, *Study of the coupling of wide band Near Field Scan probe dedicated to the investigation of the radiated immunity of Printed Circuit Boards, 23rd Workshop on Signal and Power Integrity (SPI), 2019, pp. 1–4.*
143. ANSI, *IEEE Standard Methods for Measuring Electromagnetic Field Strength of Sinusoidal Continuous Waves, 30 Hz to 30 GHz*, 1991(1991) 1–55.
144. L. EMV Technik, *Near-Field Probes*, 2022. https://www.langer-emv.de/en/category/near-field-probes/19.
145. Z. Yan, J. Wang, W. Zhang, Y. Wang, and J. Fan, *A Miniature Ultrawideband Electric Field Probe Based on Coax-Thru-Hole via Array for Near-Field Measurement*, IEEE Trans. Instrum. Meas. 66(2017) 2762–2770.
146. E. Jordan, *Electromagnetic Waves and Radiating Systems*. Prentice Hall, 1668.
147. O. Harwot, *Fast near-field characterization of integrated circuits electromagnetic interference, 21st International Conference Radioelektronika, 2011, pp. 1–4.*
148. F. Xiao, T. Takatsu, K. Murano, and Y. Kami, *Complex near electromagnetic field scanning on printed circuit board, International Symposium on Electromagnetic Compatibility - EMC EUROPE, 2012, pp. 1–4.*
149. M. H. Baharuddin, *Measurement and Characterisation of Stochastic*

Fields, Ph.D Thesis, University of Nottingham, 2019.

150. H. H. Park, J. D. Lim, H. B. Park, and J. Kim, *Near-field shielDing measurement of small shield cans in metallic mobile devices for RF interference analysis*, Electron. Lett. 52(2016) 980–982.
151. H. Rezaei *et al.*, *Source Reconstruction in Near-Field Scanning Using Inverse MoM for RFI Application*, IEEE Trans. Electromagn. Compat. 62(2020) 1628–1636.
152. J. L. Araque Quijano and G. Vecchi, *Near- and Very Near-Field Accuracy in 3-D Source Reconstruction*, IEEE Antennas Wirel. Propag. Lett., 9(2010) 634–637.
153. S. Piersanti *et al.*, *Near-Field Shielding Performances of EMI Noise Suppression Absorbers*, IEEE Trans. Electromagn. Compat., 59(2017) 654–661.
154. P. Padmanabhan, K. Hardin, and W. Smith, *Broadband measurement of near-fields for predicting far-fields for EMC applications, 2014 IEEE International Symposium on Electromagnetic Compatibility (EMC), 2014, pp. 702–706.*
155. W. Liu, Z. Yan, and Z. Min, *The Far-field Estimation for Microstrip Line Based on Near-field Scanning, 2018 12th International Symposium on Antennas, Propagation and EM Theory (ISAPE), 2018, pp. 1–4.*
156. Y. Liu, B. Ravelo, and A. K. Jastrzebski, *Time-Domain Magnetic Dipole Model of PCB Near-Field Emission*, IEEE Trans. Electromagn. Compat. 58(2016) 1561–1569.
157. J. Karpowicz, P. Bienkowski, and J. Kieliszek, *Model of the minimum requirements regarding electric and magnetic field strength measurement devices for use in the near-field occupational exposure in compliance testing with respect to the requirements of European Directive 2013/35/EU, 2016 International Symposium on Electromagnetic Compatibility - EMC EUROPE*, 2016, pp. 668–671
158. K. Jomaa, F. Ndagijimana, H. Ayad, M. Fadlallah, and J. Jomaah, *Near-field characterization for 13.56 MHz RFID antenna, 2017 International Symposium on Electromagnetic Compatibility - EMC EUROPE, 2017, pp. 1–4.*
159. S. Jog, I. Deshpande, V. Bhatnagar, A. D. Roshan, and S. Gangwal, *Analysis of the Near Field Emission from the PCB of a Car Deck Player, 2018 15th International Conference on ElectroMagnetic Interference & Compatibility (INCEMIC), 2018, pp. 1–4.*
160. H. He, P. Maheshwari, and D. J. Pommerenke, *The Development of an EM-Field Probing System for Manual Near-Field Scanning*, IEEE Trans. Electromagn. Compat. 58(2016) 356–363.
161. L. Guan, G. Maghlakelidze, X. Yan, S. Shinde, and D. Pommerenke, *Optimizing measurement SNR for weak near-field scanning applications, 2017 IEEE International Symposium on Electromagnetic Compatibility & Signal/Power Integrity (EMCSI), 2017, pp. 687–691.*
162. G. Giordanengo, M. Righero, F. Vipiana, G. Vecchi, and M. Sabbadini, *Fast Antenna Testing With Reduced Near Field Sampling*, IEEE Trans. Antennas Propag. 62(2014) 2501–2513.
163. C. Christopoulos, *Technical theme topics: Characterization of Emissions from PCBs Based on Near-field Scanning*, IEEE Electromagn. Compat. Mag. 4(2015) 67–67, 2015.
164. B.-Y. Chen, W.-C. Wang, M.-J. Guo, S.-M. Wu, C.-H. Su, and M.-S. Lin, *Investigating Simultaneous Switching Noise Distribution in Frequency Domains by Near Field Scan, 2019 Joint International Symposium on Electromagnetic Compatibility, Sapporo and Asia-Pacific International Symposium on Electromagnetic Compatibility (EMC Sapporo/APEMC), 2019, pp. 254–257.*
165. *Y. Zhao, D. W. P. Thomas, C. J. Smartt, X. Zhao, and L. Yan, Challenges of Time Domain Near Field Measurement of Complex Digital Circuit, 2019 ESA Workshop on Aerospace EMC (Aerospace EMC), 2019, pp. 1–4.*
166. D. W. P. Thomas, M. H. Baharuddin, C. Smartt, G. Gradoni, G. Tanner, and S. Creagh, *Reducing the complexity of near-field scanning of stochastic fields, 13th International Conference on Advanced Technologies, Systems and Services in Telecommunications (TELSIKS), 2017, pp. 11–14.*
167. D. W. P. Thomas *et al.*, *Near-field scanning of stochastic fields considering reduction of complexity, International Symposium on Electromagnetic Compatibility - EMC EUROPE, 2017, pp. 1–6.*
168. M. H. Baharuddin *et al.*, *Analysis of Nonstationary Emissions for Efficient Characterization of Stochastic EM Fields, 2018 International Symposium on Electromagnetic Compatibility (EMC EUROPE), 2018, pp. 208–213.*
169. A. Gil, J. Segura, and N. M. Temme, *Numerical Methods for Special Functions*. Philadelphia:Society for Industrial and Applied Mathematics, 2007.
170. M. Last and R. Shumway, *Detecting abrupt changes in a piecewise locally stationary time series*, J. Multivar. Anal. 99(2008) 191–214.
171. S. Adak, *Time-Dependent Spectral Analysis of Nonstationary Time Series*, J. Am. Stat. Assoc. 93(1998) 1488–1500.